AGU100 ADVANCING EARTH AND SPACE SCIENCE

Geophysical Research Letters

RESEARCH LETTER
10.1029/2018GL077239

Key Points:
- Urban heat island (UHI) effect reduces aerosols at urban surface considerably but increases them above the PBL and in rural area
- UHI effect increases the atmospheric instability and PBL height, favoring the dispersion of pollutants during daytime
- Urbanization-induced emission increases aerosols more than the reduction by UHI effect, with a net increase in winter haze occurrence

Supporting Information:
- Supporting Information S1

Correspondence to:
Y. Qian and B. Yang,
yun.qian@pnnl.gov;
byang@nju.edu.cn

Citation:
Zhong, S., Qian, Y., Sarangi, C., Zhao, C., Leung, R., Wang, H., et al. (2018). Urbanization effect on winter haze in the Yangtze River Delta region of China. *Geophysical Research Letters, 45*, 6710–6718. https://doi.org/10.1029/2018GL077239

Received 21 JAN 2018
Accepted 17 MAY 2018
Accepted article online 25 MAY 2018
Published online 6 JUL 2018

Urbanization Effect on Winter Haze in the Yangtze River Delta Region of China

Shi Zhong[1,2], Yun Qian[2], Chandan Sarangi[2], Chun Zhao[3], Ruby Leung[2], Hailong Wang[2], Huiping Yan[4], Tao Yang[1], and Ben Yang[5]

[1]State Key Laboratory of Hydrology-Water Resources and Hydraulic Engineering, Center for Global Change and Water Cycle, Hohai University, Nanjing, China, [2]Pacific Northwest National Laboratory, Richland, WA, USA, [3]School of Earth and Space Sciences, University of Science and Technology of China, Hefei, China, [4]College of Atmospheric Science, Nanjing University of Information Science and Technology, Nanjing, China, [5]School of Atmospheric Sciences, Nanjing University, Nanjing, China

Abstract The impact of urbanization-induced land-cover change and increase in anthropogenic emissions on the air quality of the megacity cluster of the Yangtze River Delta is investigated using the WRF-Chem model coupled with an urban canopy model at cloud-resolving resolution. The urban land-cover effect results in considerable reduction of near-surface aerosol concentrations over urban regions and an increase in particle concentrations at higher altitudes over the surrounding rural areas. The urban heat island effect increases the lower atmospheric instability and vertical velocity, thus increasing the planetary boundary layer height and ventilation over the urban area, favoring the dispersion of pollutants from urbanized areas to their immediate vicinities. However, the urbanization-induced increases in aerosol emissions outweigh that of land-cover change, resulting in a net increase in surface particle concentrations by up to 50 $\mu g\ m^{-3}$ and the occurrence of winter haze by more than 10 d $season^{-1}$ in the Yangtze River Delta region.

Plain Language Summary Urbanization can significantly impact land-cover properties, surface heating, and emissions of air pollutants. China has experienced very rapid urbanization in the past few decades. Yangtze River Delta urban region became the largest megacity cluster in the world. In this study, we use an atmospheric model to examine how the urbanization-induced changes affect the air quality in the YRD urban and surrounding rural areas. Land-cover change and associated surface heating effect provide a favorable condition for moving pollutants out of Yangtze River Delta urban areas, but the increased pollutant emissions add even more, resulting in a net increase in the occurrence of winter haze. The number of days with very poor air quality increased by up to 10 days in each winter during 2000s, compared to 1970s.

1. Introduction

Urbanization can significantly affect boundary layer micrometeorology and regional climate via changes in the surface properties, enhanced anthropogenic heating, and emissions of anthropogenic pollutants. The most discernible impact of urbanization is the urban heat island (UHI) effect that can lead to a warmer environment over urban areas than surrounding areas (Landsberg, 1981; Oke, 1982, 1987). The UHI has been well documented to change the regional climate via the modification of surface evaporation (Wienert & Kuttler, 2005) and atmospheric circulations (Lei et al., 2008; Shepherd & Burian, 2003) over and around urbanized areas (Feng et al., 2014; Inoue & Kimura, 2004; Lin et al., 2016; Miao et al., 2010; Zhong et al., 2017; Zhou et al., 2004). At the same time, human activities in the metropolitan areas consume a large amount of energy, resulting in increased emissions of pollutants and their precursors and consequently aerosol loading in the atmosphere (Han et al., 2014; Wang et al., 2006). Atmospheric aerosols have long been recognized to affect the radiative heating profiles in the atmosphere via aerosol-radiation interactions (Charlson et al., 1992; Hansen et al., 1997; McFarquhar & Wang, 2006; Qian et al., 2006, 2015; Yu et al., 2006) and affect clouds and precipitation via aerosol-cloud interactions (Fan et al., 2015; Qian et al., 2010; Rosenfeld, 2000; Rosenfeld et al., 2008; Tao et al., 2012; Zhong et al., 2015, 2017). However, particulate pollutants over urbanized area include a large fraction of fine particulate matter ($PM_{2.5}$), which directly affects both atmospheric visibility and human health (von Bismarck-Osten et al., 2013;van Dingenen et al., 2004; Han et al., 2014; Pope & Dockery, 2012).

China has been experiencing an intensive urban expansion during the past three decades, with urbanization level increasing from 20% in 1982 up to 50% in 2012 (Han et al., 2014). As one of the most developed areas in

China, the Yangtze River Delta (YRD) has become the largest metropolitan cluster in the world. The urban land-cover expansion has induced a remarkable warming due to the UHI effect, with the annual mean warming exceeding 0.16 °C/decade (Du et al., 2006; Ren et al., 2008; X. M. Wang et al., 2015; Yang et al., 2017), while several other studies suggest a smaller warming effect at the large scale (Li et al., 2004; Parker, 2006; F. Wang et al., 2015). Meanwhile, large metropolitan areas with ever-growing population are steady source regions of anthropogenic pollutants, such as sulfates, nitrates, and black carbon (Qian et al., 2001). The rapid urbanization growth has caused severe air pollution problem in the urbanized regions (Chan & Yao, 2008; Huang et al., 2009). More than three quarters of the urban population in China are exposed to poor air quality that does not meet the national standards, especially during winter time (Shao et al., 2006).

The impact of urbanization on local and regional climate via the UHI effect and aerosol emissions has been examined in previous studies (e.g., Qian & Giorgi, 1999; Qian et al., 2006, 2007; Zhong et al., 2015, 2017). Numerical modeling studies have also been performed to quantify the impact of urban expansion on air quality in eastern China (Liao et al., 2015; Tao et al., 2015), which demonstrated that urban land-cover change reduces the near-surface concentrations of $PM_{2.5}$. However, very few studies have quantified the individual and combined effects of urbanization-induced UHI and elevated emissions on pollutant particles over and around major metropolitan areas. The objective of this study is to assess the influence of urbanization-induced UHI and anthropogenic emissions on near-surface pollutant concentrations and the occurrence of winter haze events, and to better understand the underlying mechanism of urbanization-haze interaction through the changing planetary boundary layer (PBL) structure over the YRD megacity cluster of China.

2. Methodology

In this study, the WRF-Chem model (Fast et al., 2006; Grell et al., 2005; Qian et al., 2010) coupled with a single-layer urban canopy model (Chen et al., 2001; Kusaka et al., 2001) is used to simulate climate features and air quality in the YRD region. We conduct three sets of 5-year (2006–2010) simulations with a horizontal grid spacing of 3 km and 50 vertical levels extending to 50 hPa. Initial and boundary conditions for meteorological fields are derived from the National Center for Environmental Prediction FNL global reanalysis data on a 1° × 1° grid at 6-hr interval (https://rda.ucar.edu/datasets/ds083.2/). The simulations are initialized on 15 December of the previous year for each year during 2006–2010 to allow for a 16-day spin-up time and then continuously integrated for the entire year. Detailed configurations of the physical parameterization schemes used in the model can be found in Table 1 in Zhong et al. (2017).

Three experiments (i.e., "LU + Emission," "Emission," and "None") are conducted to separate the responses to aerosol and land use (LU) changes from their combined effects. "LU + Emission" experiment represents the "present" (2006) urbanization level for both land-cover and anthropogenic emissions. The dominant land-cover data set is derived from the U.S. Geological Survey 30s data set that includes 24 categories of land-cover type, except that the land cover over the urban areas is updated using the stable nighttime light product (version 4) at 1-km spatial resolution (http://ngdc.noaa.gov/eog//dmsp/downloadV4composites.html). Anthropogenic emissions of aerosols and their precursors are prescribed based on the Asian emission inventory (Zhang et al., 2009). Black carbon, organic matter, and SO_2 emissions are obtained from the China emission inventory for 2008 (Lu et al., 2011).

Figures 1a and 1b illustrate the land-cover category and anthropogenic black carbon emission fluxes for the "LU + Emission" simulation, respectively. They show that areas with strong emissions are mainly located in city clusters such as Shanghai (SH), Hangzhou, and Suzhou-Wuxi-Changzhou, all within the megacity belt. The "Emission" simulation uses the present aerosol emission data but with the land cover of the 1970s. In the "None" experiment, both land cover and emissions are set to the conditions of the 1970s. The differences between LU + Emission and Emission, Emission and None, and LU + Emission and None are used to derive the effect of urban land-cover change, anthropogenic emissions, and their combined effect, respectively. The impact of urbanization on air pollution is investigated only in boreal winter (December, January, and February), which is the season when persistent haze pollution episodes in cities are more likely to develop (Birmili & Hoffmann, 2006; Chen & Wang, 2015). To evaluate the model results, the wintertime near-surface temperature and precipitation from the LU + Emission simulation are compared with the meteorological station observations for 2006–2010 (Figure S1 in the supporting information). The simulated spatial pattern of near-surface air temperature agrees well with the observations, with warmer temperatures in the YRD

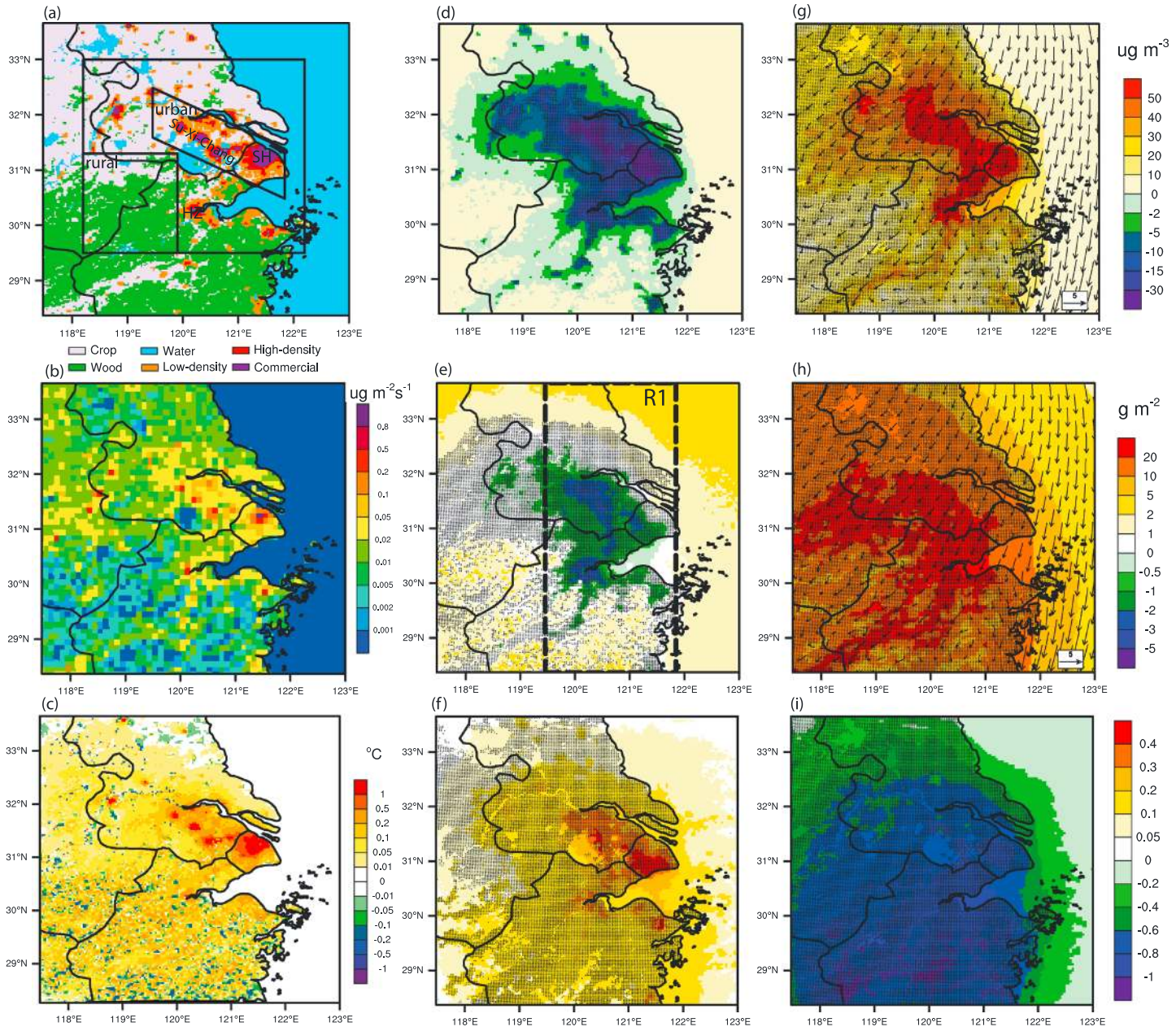

Figure 1. Spatial distributions of (a) land use categories for year 2006; (b) black carbon (BC) emission rates (units: $\mu g\ m^{-2}\ s^{-1}$) averaged over 2006–2010; (c) differences in annual 2-m temperature (units: °C) between simulations "LU + Emission" and "emission"; (d and g) differences in $PM_{2.5}$ mass concentration at the surface (units: $\mu g\ m^{-3}$) between simulations "LU + Emission" and "Emission" and between "Emission" and "None," respectively, with the near-surface winds simulated in "None" superimposed. (e and h) The same as (d) and (g), but for column-integrated $PM_{2.5}$ mass (units: $g\ m^{-2}$). (f and i) The same as (d) and (g), but for the ratio of integrated $PM_{2.5}$ above 500 m to that below 500 m. The stippled (black dots) areas have statistically significant changes. The boxes in (a) outline the urban and downwind rural regions over which further analyses are conducted, and box R1 in (e) marks the cross-sectional area analyzed.

megacity cluster region. The model also captures the observed precipitation distribution except for an underestimation over the southern part of the domain.

3. Urbanization Impact on Pollutant Distribution

Distinct land-cover change effect on 2-m air temperature (T_{2m}) can be seen in Figure 1c, showing an average temperature increase of about 0.53 °C in urban areas and 0.96 °C in commercial areas as delineated in Figure 1a. A maximum increase is observed in SH, where the temperature increases by 1.27 °C. Figure 1d

shows the difference in surface $PM_{2.5}$ mass concentration between the "LU + Emission" and "Emission" simulations, representing the urban land-cover effect that induces a significant decrease in surface $PM_{2.5}$ concentrations over urban and peripheral suburban areas. A maximum reduction (~43 $\mu g\ m^{-3}$) is found over SH. The downwind rural regions only show marginal reductions. Urban land-cover change also affects the vertical distribution of aerosols (Figures 1e and 1f). As a result, the ratio of the integrated $PM_{2.5}$ mass above 500 m to that below 500 m increases over the entire domain of study. Specifically, the ratio is increased by ~30–40% and ~10% (Figure 1f) over the urban and rural areas, respectively, suggesting the presence of more air pollutants at higher altitudes compared to lower atmosphere. As the PBL height (PBLH) is lower than 500 m in our simulation (not shown), we infer that more aerosol particles are lifted above the PBL due to the land-cover change.

For clarity, Figure S2 illustrates the simulated vertical distributions of $PM_{2.5}$ and PM_{10} mass concentration for all three simulations over urban and rural regions. Over urban regions, the $PM_{2.5}$ mass is largely reduced below 500 m but increased above 500 m (Figure S2a) due to the urban land-cover change. For the rural area, however, $PM_{2.5}$ mass concentrations increase only above 500 m (Figure S2c). Thus, the urban land-cover effect tends to transport more pollutants upward over the urban areas. The difference plot (Figure 1e) shows a reduction in the column-integrated $PM_{2.5}$ mass (up to 4.23 $g\ m^{-2}$) over the megacity belt due to the land-cover change. In contrast, over the rural areas, the column-integrated $PM_{2.5}$ only increases slightly (up to 1.5 $\mu g\ m^{-2}$). According to Figure S2, the urban land-cover associated decrease (increase) in column mass of particles over the urban (rural) areas is mainly due to the decrease (increase) below (above) 500 m. Consistent with the prevailing monsoon circulation, northeasterly dominates the YRD in winter (Figure 1g). The prominent increase in air pollutants only occurs in the free troposphere downwind (southwestern) of the city clusters, indicating the transport of uplifted aerosols from the megacity belt by the prevailing northwesterly.

Figures 1g–1i show the differences in surface $PM_{2.5}$ mass concentration, column-integrated $PM_{2.5}$, and aerosol vertical distribution, respectively, between the "Emission" and the "None" simulations. As expected, increased anthropogenic emissions increase the near-surface and the column-integrated $PM_{2.5}$ concentration not only over the urbanized areas but also almost over the entire simulation domain (Figures 1g–1i). The increase in pollutants has a maximum in the lower atmosphere of the megacity belt (Figure 1h). Comparison between Figures 1d and 1g and 1f and 1i shows that the absolute change in $PM_{2.5}$ mass concentration attributed to pollutant emissions is more striking than that due to urban land-cover change. Therefore, the net urbanization impact is dominated by aerosol emissions, resulting in a net increase in pollutant concentrations, both at the surface and over the entire column, in the YRD region (not shown).

As is well established, the most discernible impact of urban land-cover change, that is, the UHI effect, tends to warm the environment and further modify the atmospheric circulations. To confirm that the changes in aerosol spatial distribution are induced by the urban land-cover effect (seen in Figures 1 and S2), we plot the changes in vertical profiles of $PM_{2.5}$ mass concentration (Figure 2a) over urban and downwind rural areas (according to Figure 1a) in the daytime and nighttime, respectively, due to land-cover effect. The $PM_{2.5}$ mass concentration below 500 m is reduced over urbanized area with a maximum reduction of 13.70 and 3.79 $\mu g\ m^{-3}$ during daytime and nighttime, respectively. In the rural area, a maximum increase in $PM_{2.5}$ concentrations (~4 $\mu g\ m^{-3}$) is observed around 1,000 m during daytime. The nighttime changes follow similar a pattern as daytime, but with smaller magnitudes.

Figures 2b and 2d illustrate the UHI effect on the vertical profiles of potential temperature, vertical velocity, and divergence over urban and rural areas. During the daytime, potential temperature increases near the surface but decreases at higher altitudes over urbanized area, which indicates a decrease in atmospheric stability in urbanized area. By contrast, the low-level atmospheric stability increases in rural area during the daytime. Likewise, the lower tropospheric vertical velocity also increases dramatically with maximum values around 400 m (see Figure 2c) over urbanized area in the daytime. In addition, the urban land-cover effect also favors daytime convergence below 500 m (see Figure 2d) and divergence above. On the contrary, over rural area, the urban land-cover effect causes a reduction in the vertical velocity along with enhanced divergence below 500 m and increased convergence above. During nighttime, however, the UHI impact on vertical velocity and divergence is small.

Figure S3 shows the diurnal cycle of the urban land-cover effect on 2-m temperature, sensible heat flux, PBLH, and surface $PM_{2.5}$ mass concentration over urban area (shown in Figure 1a). The difference in 2-m

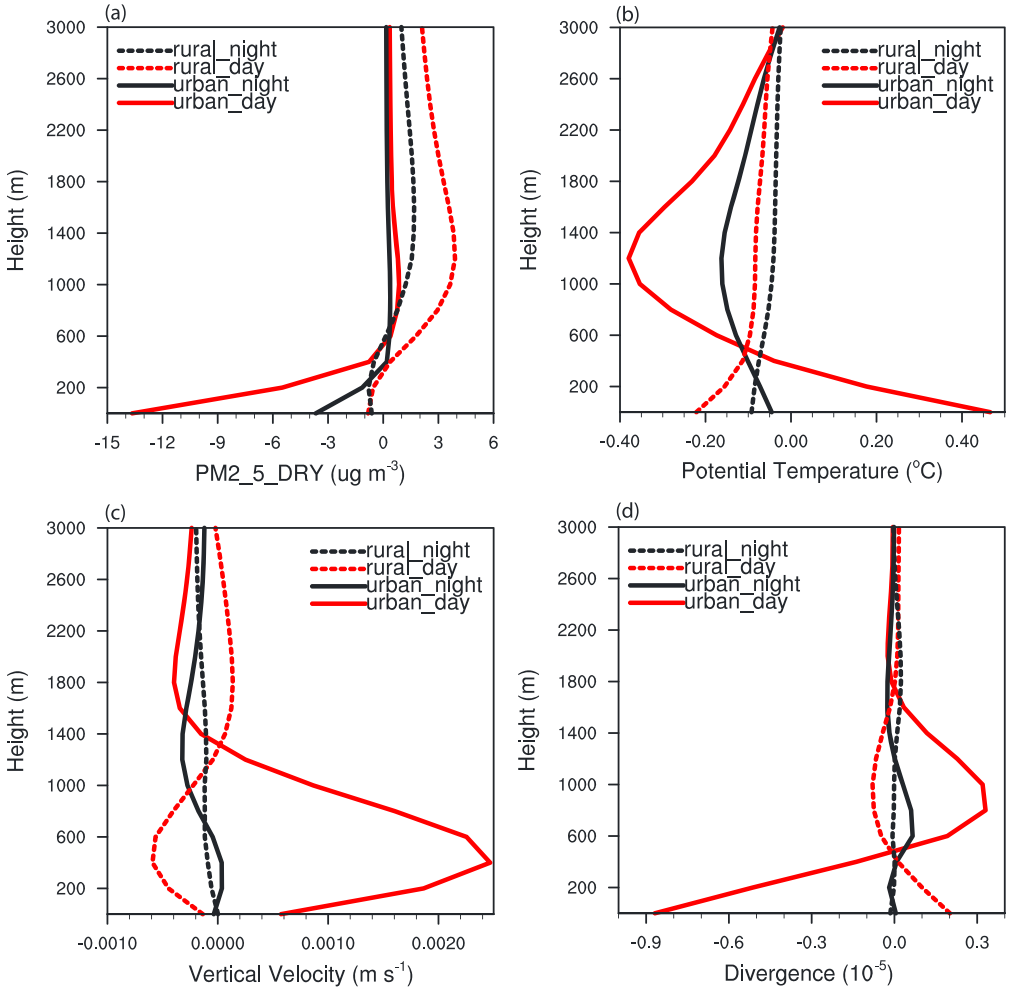

Figure 2. Differences in vertical profiles of (a) $PM_{2.5}$ mass concentration (units: μg m^{-3}), (b) potential temperature (units: °C), (c) vertical velocity (units: m s^{-1}), and (d) divergence (units: 10^{-5}) for urban (solid line) and rural area (dashed line) in the daytime (red line) and nighttime (black line)between simulations "LU + Emission" and "Emission."

temperature is positive starting from 0600 LST and increases gradually until reaching a maximum value of 0.93 °C at 1700 LST. However, the temperature decreases slightly from 2000 LST to early morning. Such a nighttime cooling effect is also found in satellite observation (Figure S4). In our simulations, there are three urban categories, that is, commercial, high-density residential, and low-density residential area (Figure 1a). Negative UHI effect at nighttime only occurs in the latter two categories where anthropogenic heating is much weaker than in commercial area. The LU change in the low-density residential area leads to lower skin temperature but higher sensible heat and upward longwave radiation flux during daytime, indicating a greater surface energy loss to the atmosphere due to increased surface roughness and emissivity in urban canopy. Therefore, the daytime energy storage deceases in the subsurface, which limits the upward ground flux and accelerates the cooling after sunset in the low-density residential area.

Consistent with 2-m temperature, the surface sensible heat flux and PBLH (Figures S3b and S3c) also increase gradually from 0600 LST and reach a maximum during afternoon, followed by a drop till 0600 LST. However, the PBLH is increased throughout the entire day despite the negative UHI near the surface during nighttime. In accordance, the surface $PM_{2.5}$ (Figure S3d) decreases due to the land-cover change, especially during the daytime. The magnitude of reduction in $PM_{2.5}$ increases gradually from 0000 LST and reaches a peak reduction of −30.58 μg m^{-3} at 1400 LST. Overall the magnitude of UHI effect and its induced changes in aerosol over YRD dominate during the daytime over the smaller changes during nighttime.

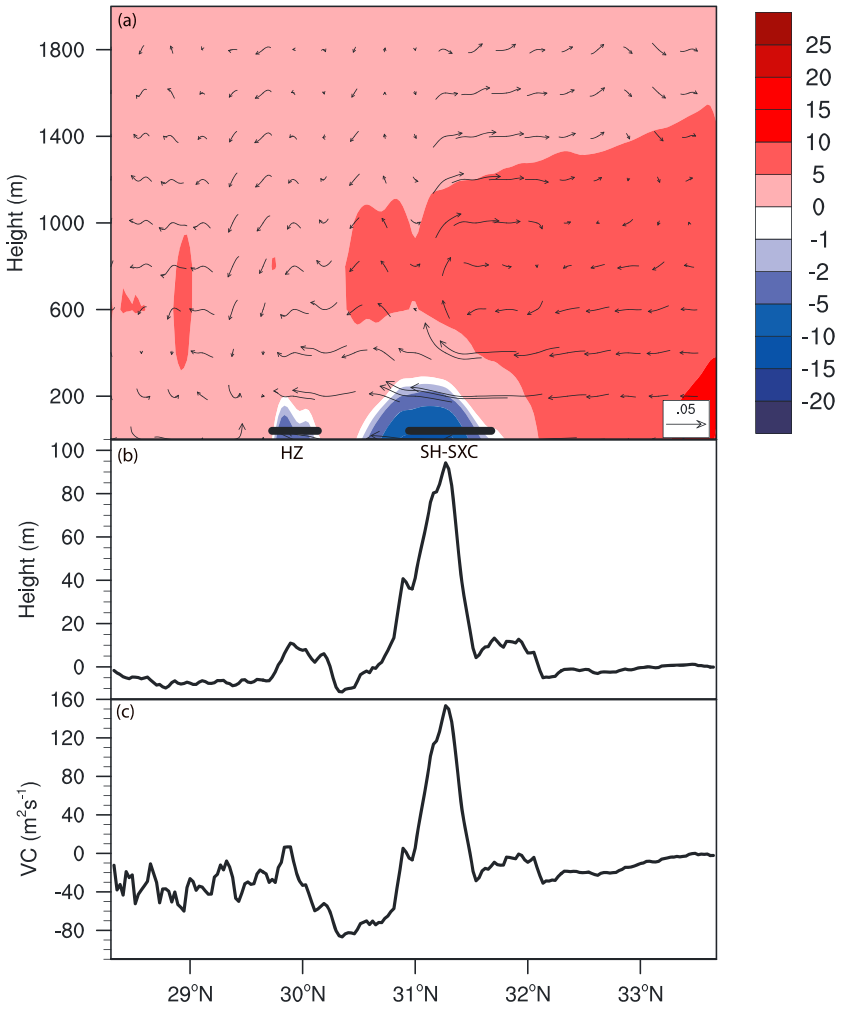

Figure 3. Latitude-height plot of the differences in (a) wind vectors (units: m s^{-1}) and $PM_{2.5}$ mass concentration (shaded; units: μg m^{-3}), (b) planetary boundary layer height (units: m), and (c) ventilation coefficient (units: m^2 s^{-1}) between simulations "LU + Emission" and "Emission" in the daytime.

Collocated UHI effects on wind vector and $PM_{2.5}$ concentrations over region R1 (Figure 1e) during daytime are shown in Figure 3. Consistent with the aerosol vertical distribution, modification of the wind circulation suggests that pollutants emitted in urban region can be lifted from the near surface and transported to the immediate vicinities. As a result, the $PM_{2.5}$ concentrations decrease dramatically below 200 m over urban areas, with a maximum reduction of 11.28 μg m^{-3}. On the contrary, there is a slight increase in $PM_{2.5}$ concentrations over rural areas. The ventilation coefficient (VC) over R1 during daytime is estimated using Equation (1), where *U* is the mean horizontal wind speed within PBL (Ashrafi et al., 2009):

$$VC = PBLH^{*} U \quad (1)$$

Higher VC value indicates potentially stronger dilution of air pollutants at the surface (Sujatha et al., 2016). Figure 3 clearly shows that both the mean PBLH and *U* increase over urbanized area in the YRD (i.e. SH, Suzhou-Wuxi-Changzhou, and Hangzhou), with a peak increase of PBLH reaching 92.74 m. Thus, the VC increases in urbanized area and decreases slightly over rural area, supporting our argument of increased transport efficiency of pollutants from urban area to the peripheral region.

Extreme haze episodes repeatedly shrouded the megacities of China in recent years, with atmospheric visibility reduced down to 100 m (Chan & Yao, 2008; Wang et al., 2014). Extreme haze pollution not only disrupts transportation services (e.g., closed highways and canceled flights) but also causes major environmental and

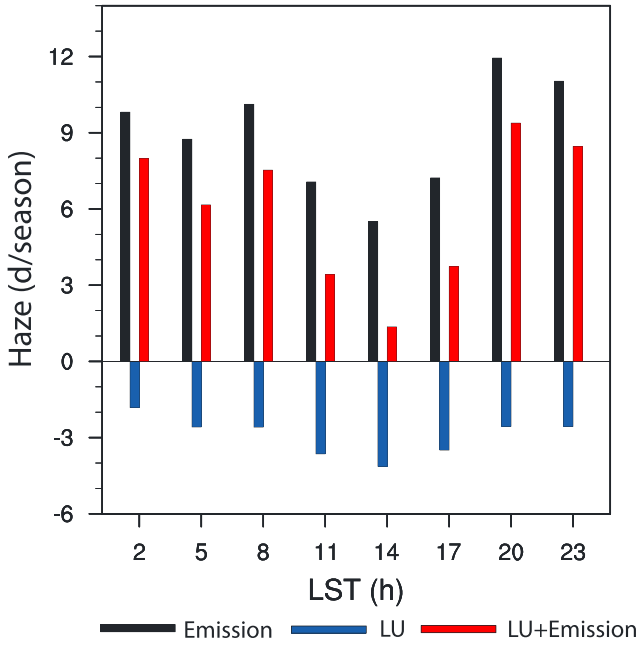

Figure 4. Diurnal cycle of the difference in haze occurrence between simulations "Emission" and "None" (black bar), "LU + Emission" and "Emission" (blue bar), and "LU + Emission" and "None" (red bar), respectively, over urbanized area.

health problems. Figure 4 illustrates the changes in diurnal cycle of haze occurrence over urbanized areas due to anthropogenic emissions and/or land-cover effect. By definition, a haze event occurs when the visibility is less than 10 km and relative humidity is less than 90% (Quan et al., 2011). The visibility is calculated as follows:

$$\mathrm{VIS} = 3.912/\beta \tag{2}$$

where β refers to the total optical extinction coefficient due to aerosol particles and/or cloud droplets. We can see that the anthropogenic emissions induced by urbanization substantially increase the occurrence of haze days, especially during the nighttime by about 10 d season^{-1}, due to weak mixing and dispersion. The maximum relative change of haze occurrence is observed at 1700 LST, with a value of over 200%. In contrast, the urban land-cover change exerts an opposite impact on the frequency of haze days, reducing it by up to 50%. The reduction of haze events due to land-cover change effect is highest during late afternoon (1400–2000 LST) when UHI effect is most prominent (shown in Figure S3a). The mechanistic understanding gained from this study suggests that good air quality and haze free conditions can be achieved more effectively within the megacity belt by reducing the present emissions because the UHI effect can offset almost half of the enhancement in haze events associated with the present increase in emissions.

4. Summary

The WRF-Chem model coupled with a single-layer urban canopy model is employed to investigate the influences of urbanization-induced land-cover change and increase in anthropogenic emissions on aerosol concentrations in the YRD during winter season. As expected, the increased anthropogenic emissions increase the $PM_{2.5}$ concentration dramatically over the urbanized areas and the downwind rural regions. In contrast, the urban land-cover effect leads to a decrease in surface and lower tropospheric $PM_{2.5}$ concentrations over the megacity belt and peripheral regions. Moreover, due to the urban land-cover effect, the ratio of $PM_{2.5}$ mass above 500 m to that below 500 m is increased by up to 40% and 10% over the megacity belt and downwind rural regions, respectively. Such changes in the ratio indicate that the urban land-cover effect can redistribute pollutants from the lower troposphere of megacities to higher altitudes and broader areas. As a result, the column-integrated $PM_{2.5}$ mass increases over the downwind rural areas, mainly above 500 m.

Our analysis also shows that these changes in pollutants over YRD associated with urban land-cover change are prevalent mainly in daytime, during which atmospheric instability and convergence below 500 m and divergence above all increase. As a result, the increased vertical velocity and ventilation over urban areas tend to lift the boundary-layer aerosol particles higher to be transported by prevailing winds to surrounding rural areas. However, the increase in aerosol emissions outweighs the UHI effect, resulting in a net increase in particle concentrations (up to 50 $\mu g\ m^{-3}$) and haze days (up to 200%) over the entire YRD region due to urbanization. Nevertheless, the UHI effect can offset up to 50% of the increase in haze events.

Acknowledgments
This study was supported by the U.S. Department of Energy (DOE)'s office of Science Biological and Environmental Research as part of the Regional and Global Climate Modeling Program. The Pacific Northwest National Laboratory (PNNL) is operated for DOE by Battelle Memorial Institute under contract DE-AC05-76RL01830. S.Z. acknowledges the support by the "Fundamental Research Funds for the Central Universities" (grant 2017B10614) and the China Postdoctoral Science Foundation (grant 2017M611666). C.Z. was supported by the "Thousand Talents Plan for Young Professionals" program and the "Fundamental Research Funds for the Central Universities" of China. This study used computing resources from the PNNL Institutional Computing (PIC) and the National Energy Research Scientific Computing Center (NERSC) at Lawrence Berkeley National Laboratory. The model outputs and meteorological station data used in this study are publicly available in Github repository at https://github.com/brady1234/wrfout_urban-haze.

References

Ashrafi, K., Shafie-Pour, M., & Kamalan, H. (2009). Estimating temporal and seasonal variation of ventilation coefficients. *International Journal of Environmental Research*, *3*, 637–644.

Birmili, W., & Hoffmann, T. (2006). Particulate and dust pollution, inorganic and organic compounds. *Encyclopedia ofRespiratory Medicine*, *8*(3), 110–120.

Chan, C., & Yao, X. (2008). Air pollution in mega cities in China. *Atmospheric Environment*, *42*(1), 1–42. https://doi.org/10.1016/j.atmosenv.2007.09.003

Charlson, R. J., Schwarts, S. E., Hales, J. M., Cess, R. D., Coakley, J. A., Hansen, J. E., & Hofmann, D. J. (1992). Climate forcing by anthropogenic aerosols. *Science*, *255*(5043), 423–430. https://doi.org/10.1126/science.255.5043.423

Chen, F., Kusaka, H., Bornstein, R., Ching, J., Grimmond, C. S. B., Grossman-Clarke, S., & Zhang, C. L. (2001). The integrated WRF/urban modeling system: Development, evaluation, and applications to urban environmental problems. *International Journal of Climatology*, *31*, 273–288.

Chen, H., & Wang, H. (2015). Haze days in North China and the associated atmospheric circulations based on daily visibility data from 1960 to 2012. *Journal of Geophysical Research: Atmospheres*, *120*, 5895–5909. https://doi.org/10.1002/2015JD023225

Du, Y., Xie, Z. Q., Zeng, Y., Shi, Y. F., & Wu, J. G. (2006). Impact of urban expansion on regional temperature change in the Yangtze River Delta. *Acta Geophysica Sinica*, *17*, 387–398.

Fan, J., Rosenfeld, D., Yang, Y., Zhao, C., Leung, Y. R., & Li, Z. (2015). Substantial contribution of anthropogenic air pollution to catastrophic floods in Southwest China. *Geophysical Research Letters*, *42*, 6066–6075. https://doi.org/10.1002/2015GL064479

Fast, J. D., Gustafson, W. I. Jr., Easter, R. C., Zaveri, R. A., Barnard, J. C., Chapman, E. G., et al. (2006). Evolution of ozone, particulates, and aerosol direct forcing in an urban area using a new fully-coupled meteorology, chemistry, and aerosol model. *Journal of Geophysical Research*, *111*, D21305. https://doi.org/10.1029/2005JD006721

Feng, J., Wang, J., & Yan, Z. (2014). Impact of anthropogenic heat release on regional climate in three vast urban agglomerations in China. *Advances in Atmospheric Sciences*, *31*(2), 363–373. https://doi.org/10.1007/s00376-013-3041-z

Grell, G. A., Peckham, S. E., Schmitz, R., Mckeen, S. A., Frost, G., Skamarock, W. C., & Eder, B. (2005). Fully coupled "online" chemistry within the WRF model. *Atmospheric Environment*, *39*(37), 6957–6975. https://doi.org/10.1016/j.atmosenv.2005.04.027

Han, L., Zhou, W., Li, W., & Li, L. (2014). Impact of urbanization level on urban air quality: A case of fine particles (PM 2.5) in Chinese cities. *Environmental Pollution*, *194*, 163–170. https://doi.org/10.1016/j.envpol.2014.07.022

Hansen, J., Sato, M., & Ruedy, R. (1997). Radiative forcing and climate response. *Journal of Geophysical Research*, *102*(D6), 6831–6864. https://doi.org/10.1029/96JD03436

Huang, W., Tan, J., Kan, H., Zhao, N., Song, W., Song, C., et al. (2009). Visibility, air quality and daily mortality in Shanghai, China. *Science of the Total Environment*, *407*(10), 3295–3300. https://doi.org/10.1016/j.scitotenv.2009.02.019

Inoue, T. F., & Kimura, F. (2004). Urban effects on low-level clouds around the Tokyo metropolitan area on clear summer days. *Geophysical Research Letters*, *31*, L05103. https://doi.org/10.1029/2003GL018908

Kusaka, H., Kikegawa, Y., & Kimura, F. (2001). A simple single layer urban canopy model for atmospheric models: Comparison with multi-layer and slab models. *Boundary-Layer Meteorology*, *101*(3), 329–358. https://doi.org/10.1023/A:1019207923078

Landsberg, H. E. (1981). *The urban climate*. Londen, UK: Academic Press.

Lei, M., Niyogi, D., Kishtawal, C., Pielke, R. A. Sr., Beltrán- Przekurat, A., Nobis, T. E., & Vaidya, S. S. (2008). Effect of explicit urban land surface representation on the simulation of the 26 July 2005 heavy rain event over Mumbai, India. *Atmospheric Chemistry and Physics*, *8*(20), 5975–5995. https://doi.org/10.5194/acp-8-5975-2008

Li, Q., Zhang, H., Liu, X., & Huang, J. (2004). Urban heat island effect on annual mean temperature during the last 50 years in China. *Theoretical and Applied Climatology*, *79*(3–4), 165–174. https://doi.org/10.1007/s00704-004-0065-4

Liao, J., Wang, T., Jiang, Z., Zhuang, B., Xie, M., Yin, C., et al. (2015). WRF/Chem modeling of the impacts of urban expansion on regional climate and air pollutants in Yangtze River Delta, China. *Atmospheric Environment*, *106*, 204–214. https://doi.org/10.1016/j.atmosenv.2015.01.059

Lin, S., Feng, J., Wang, J., & Hu, Y. (2016). Modeling the contribution of long-term urbanization to temperature increase in three extensive urban agglomerations in China. *Journal of Geophysical Research: Atmospheres*, *121*, 1683–1697. https://doi.org/10.1002/2015JD024227

Lu, Z., Zhang, Q., & Streets, D. G. (2011). Sulfur dioxide and primary carbonaceous aerosol emissions in China and India, 1996–2010. *Atmospheric Chemistry and Physics*, *11*(18), 9839–9864. https://doi.org/10.5194/acp-11-9839-2011

McFarquhar, G. M., & Wang, H. (2006). Effects of aerosols on trade wind cumuli over the Indian Ocean: Model simulations. *Quarterly Journal of the Royal Meteorological Society*, *132*(616), 821–843. https://doi.org/10.1256/qj.04.179

Miao, S. G., Chen, F., Li, Q. C., & Fan, S. Y. (2010). Impacts of urban processes and urbanization on summer precipitation: A case study of heavy rainfall in Beijing on 1 August 2006. *Journal of Applied Meteorology and Climatology*, *50*, 806–825.

Oke, T. R. (1982). The energetic basis of the urban heat island. *Quarterly Journal of the Royal Meteorological Society*, *108*, 1–22.

Oke, T. R. (1987). *Boundary layer climates*, (2nd ed., p. 435). London, UK: Methuen Co.

Parker, D. E. (2006). A demonstration that large-scale warming is not urban. *Journal of Climate*, *19*(12), 2882–2895. https://doi.org/10.1175/JCLI3730.1

Pope, C. A. III, & Dockery, D. (2012). Health effects of fine particle air pollution: Lines that connect. *Journal of the Air and Waste Management Association*, *56*, 709–742.

Qian, Y., & Giorgi, F. (1999). Interactive coupling of regional climate and sulfate aerosol models over East Asia. *Journal of Geophysical Research*, *104*(D6), 6477–6499. https://doi.org/10.1029/98JD02347

Qian, Y., Giorgi, F., Huang, Y., Chameides, W. L., & Luo, C. (2001). Regional simulation of anthropogenic sulfur over East Asia and its sensitivity to model parameters. *Tellus Series B: Chemical and Physical Meteorology*, *53*(2), 171–191. https://doi.org/10.1034/j.1600-0889.2001.d01-14.x

Qian, Y., Gustafson, W. I. Jr., & Fast, J. D. (2010). An investigation of the sub-grid variability of trace gases and aerosols for global climate modeling. *Atmospheric Chemistry and Physics*, *10*(14), 6917–6946. https://doi.org/10.5194/acp-10-6917-2010

Qian, Y., Kaiser, D. P., Leung, L. R., & Xu, M. (2006). More frequent cloud-free sky and less surface solar radiation in China from 1955 to 2000. *Geophysical Research Letters*, *33*, L01812. https://doi.org/10.1029/2005GL024586

Qian, Y., Wang, W., Leung, L. R., & Kaiser, D. P. (2007). Variability of solar radiation under cloud-free skies in China: The role of aerosols. *Geophysical Research Letters*, *34*, L12804. https://doi.org/10.1029/2006GL028800

Qian, Y., Yasunari, T. J., Doherty, S. J., Flanner, M. J., Lau, W. K. M., Jing, M., et al. (2015). Light-absorbing particles in snow and ice: Measurement and modeling of climatic and hydrological impact. *Advances in Atmospheric Sciences*, *32*(1), 64–91. https://doi.org/10.1007/s00376-014-0010-0

Quan, J., Zhang, Q., He, H., Liu, J., Huang, M., & Jin, H. (2011). Analysis of the formation of fog and haze in North China Plain (NCP). *Atmospheric Chemistry and Physics*, *11*(15), 8205–8214. https://doi.org/10.5194/acp-11-8205-2011

Ren, G., Zhou, Y., Chu, Z., Zhou, J., Zhang, A., Guo, J., & Liu, X. (2008). Urbanization effects on observed surface air temperature trends in North China. *Journal of Climate*, *21*(6), 1333–1348. https://doi.org/10.1175/2007JCLI1348.1

Rosenfeld, D. (2000). Suppression of rain and snow by urban and industrial air pollution. *Science*, *287*(5459), 1793–1796. https://doi.org/10.1126/science.287.5459.1793

Rosenfeld, D., Lohmann, U., Raga, G. B., ODowd, C. D., Kulmala, M., Fuzzi, S., et al. (2008). Flood or drought: How do aerosols affect precipitation? *Science*, *321*(5894), 1309–1313. https://doi.org/10.1126/science.1160606

Shao, M., Tang, X. Y., Zhang, Y. H., & Li, W. J. (2006). City clusters in China: Air and surface water pollution. *Frontiers in Ecology and the Environment*, *4*(7), 353–361. https://doi.org/10.1890/1540-9295(2006)004[0353:CCICAA]2.0.CO;2

Shepherd, J. M., & Burian, S. J. (2003). Detection of urban-induced rainfall anomalies in a major coastal city. *Earth Interactions*, *7*(4), 1–17. https://doi.org/10.1175/1087-3562(2003)007<0001:DOUIRA>2.0.CO;2

Sujatha, P., Mahalakshmi, D. V., Ramiz, A., Rao, P. V. N., & Naidu, C. V. (2016). Ventilation coefficient and boundary layer height impact on urban air quality. *Cogen Environmental Science*, *2*, 1125284.

Tao, W., Liu, J., Ban-Weiss, G. A., Hanglustaine, D. A., Zhang, L., Zhang, Q., et al. (2015). Effects of urban land expansion on the regional meteorology and air quality of eastern China. *Atmospheric Chemistry and Physics*, *15*(15), 8597–8614. https://doi.org/10.5194/acp-15-8597-2015

Tao, W. K., Chen, J. P., Li, Z., Wang, C., & Zhang, C. (2012). Impact of aerosols on convective clouds and precipitation. *Reviews of Geophysics*, *50*, RG2001. https://doi.org/10.1029/2011RG000369

van Dingenen, R., Raes, R. F., Putaud, J. P., Baltensperger, U., Charron, A., Facchini, M. C., et al. (2004). A European aerosol phenomenologye1: Physical characteristics of particulate matter at kerbside, urban, rural and background sites in Europe. *Atmospheric Environment*, *38*(16), 2561–2577. https://doi.org/10.1016/j.atmosenv.2004.01.040

von Bismarck-Osten, C., Birmili, W., Ketzel, M., Massling, A., Petaja, T., & Weber, S. (2013). Characterization of parameters influencing the spatio-temporal variability of urban aerosol particle number size distributions in four European cities. *Atmospheric Environment*, *77*, 415–429. https://doi.org/10.1016/j.atmosenv.2013.05.029

Wang, F., Ge, Q., Wang, S., Li, Q., & Jones, P. D. (2015). A new estimation of Urbanization's contribution to the warming trend in China. *Journal of Climate*, *28*(22), 150804114817003.

Wang, X. M., Sun, X. G., Tang, J. P., & Yang, X. Q. (2015). Urbanization-induced regional warming in Yangtze River Delta: Potential role of anthropogenic heat release. *International Journal of Climatology*, *35*(15), 4417–4430. https://doi.org/10.1002/joc.4296

Wang, Y., Yao, L., Wang, L., Liu, Z., Ji, D., Tang, G., et al. (2014). Mechanism for the formation of the January 2013 heavy haze pollution episode over central and eastern China. *Science China Earth Sciences*, *57*(1), 14–25. https://doi.org/10.1007/s11430-013-4773-4

Wang, Y., Zhuang, G., Zhang, X., Huang, K., Xu, C., Tang, A., & An, Z. (2006). The ion chemistry, seasonal cycle, and sources of PM2.5 and TSP aerosol in Shanghai. *Atmospheric Environment*, *40*(16), 2935–2952. https://doi.org/10.1016/j.atmosenv.2005.12.051

Wienert, U., & Kuttler, W. (2005). The dependence of the urban heat island intensity on latitude—A statistical approach. *Meteorologische Zeitschrift*, *14*(5), 677–686. https://doi.org/10.1127/0941-2948/2005/0069

Yang, X., Leung, L. R., Zhao, N., Zhao, C., Qian, Y., Hu, K., et al. (2017). Contribution of urbanization to the increase of extreme heat events in an urban agglomeration in East China. *Geophysical Research Letters*, *44*, 6940–6950. https://doi.org/10.1002/2017GL074084

Yu, H., Kaufman, Y. J., Chin, M., Feingold, G., Remer, L. A., Anderson, T. L., et al. (2006). A review of measurement-based assessments of the aerosol direct radiative effect and forcing. *Atmospheric Chemistry and Physics*, *6*(3), 613–666. https://doi.org/10.5194/acp-6-613-2006

Zhang, Q., Streets, D. G., Carmichael, G. R., He, K. B., Huo, H., Kannari, A., et al. (2009). Asian emissions in 2006 for the NASA INTEX-B mission. *Atmospheric Chemistry and Physics*, *9*(14), 5131–5153. https://doi.org/10.5194/acp-9-5131-2009

Zhong, S., Qian, Y., Zhao, C., Leung, R., Wang, H. L., Yang, B., et al. (2017). Urbanization-induced urban heat island and aerosol effects on climate extremes in the Yangtze River Delta region of China. *Atmospheric Chemistry and Physics*, *17*(8), 5439–5457. https://doi.org/10.5194/acp-17-5439-2017

Zhong, S., Qian, Y., Zhao, C., Leung, R., & Yang, X. Q. (2015). A case study of urbanization impact on summer precipitation in the Greater Beijing Metropolitan Area: Urban heat island versus aerosol effects. *Journal of Geophysical Research: Atmospheres*, *120*, 10,903–10,914. https://doi.org/10.1002/2015JD023753

Zhou, L., Dickinson, R. E., Tian, Y., Fang, J., Li, Q., Kaufmann, R., et al. (2004). Evidence for a significant urbanization effect on climate in China. *Proceedings of the National Academy of Sciences of the USA*, *101*(26), 9540–9544. https://doi.org/10.1073/pnas.0400357101